Nonlinear ac stationary response and dynamic magnetic hysteresis of quantum uniaxial superparamagnets

Yuri P. Kalmykov,[1] Serguey V. Titov,[2] and William T. Coffey[3]

[1]*Laboratoire de Mathématiques et Physique (LAMPS, EA 4217), Université de Perpignan Via Domitia, 52, Avenue de Paul Alduy, 66860 Perpignan Cedex, France*

[2]*Kotel'nikov Institute of Radioengineering and Electronics of the Russian Academy of Sciences, Vvedenskii Square 1, Fryazino, 141190, Russian Federation*

[3]*Department of Electronic and Electrical Engineering, Trinity College, Dublin 2, Ireland*

(Received 8 July 2015; published xxxxxx)

The nonlinear ac stationary response of uniaxial paramagnets and superparamagnets—nanoscale solids or clusters with spin number $S \sim 10^0-10^4$—in superimposed uniform ac and dc bias magnetic fields of arbitrary strength, each applied along the easy axis of magnetization, is determined by solving the evolution equation for the reduced density matrix represented as a *finite* set of three-term differential-recurrence relations for its *diagonal* matrix elements. The various harmonic components arising from the nonlinear response of the magnetization, dynamic magnetic hysteresis loops, etc., are then evaluated via matrix continued fractions indicating a pronounced dependence of the response on S arising from the quantum spin dynamics, which differ markedly from the magnetization dynamics of classical nanomagnets. In the linear response approximation, the results concur with existing solutions.

DOI: 10.1103/PhysRevB.00.004400 PACS number(s): 75.45.+j, 75.40.Gb, 75.60.−d, 75.20.−g

I. INTRODUCTION

Nanomagnetism is a rapidly expanding area of research with many novel applications particularly in information storage [1] and in medicine, e.g., in hyperthermia occasioned by induction heating of nanoparticles [2,3]. Here single-domain ferromagnetic particles exhibit essentially classical behavior while smaller entities such as free nanoclusters made of many atoms, molecular clusters, and single-molecule magnets exhibit pronounced quantum effects. Now, due to their large magnetic dipole moment [$\sim 10-10^5$ Bohr magnetons (μ_B)], the magnetization relaxation of nanomagnets driven by an ac field will exhibit a pronounced field and frequency dependence which is significant in diverse physical applications. These include nonlinear dynamic susceptibilities [4–7], stochastic resonance [8], the dynamic magnetic hysteresis [9–12], etc. In general, however, the nonlinear response to an external field invariably poses a difficult problem because that response will always depend on the *precise* nature of the stimulus. Thus, no *unique* response function valid for all stimuli exists unlike in the linear response to a weak magnetic field. These difficulties are compounded in quantum spin systems such as molecular magnets and nanoclusters, where both the field and frequency dependence of the dynamic response to an ac driving field (which is our main concern here) differ profoundly from their classical counterparts due to tunneling effects [4].

In the context of linear response theory, spin relaxation of nanomagnets for arbitrary spin number S was usually treated via the evolution equation for the spin-density matrix using the second order of perturbation theory in the spin-bath coupling (see, e.g., [13–17]). In particular, Garanin [13] and García-Palacios *et al.* [16] gave a concise treatment of the longitudinal spin relaxation of *uniaxial* superparamagnets by proceeding from the quantum Hubbard operator representation of the evolution equation for the spin-density matrix. This problem has also been treated [18–20] via the master equation for the distribution function of spin orientations in the representation (phase) space of the polar and azimuthal angles that is completely analogous [21–24] to the treatment of relaxation of classical spins via the Fokker-Planck equation governing the evolution of the distribution function of spin orientations [25]. An important result of all these studies is that one can now accurately evaluate quantum effects in the linear dynamic susceptibility, signal-to-noise ratio in the stochastic resonance, etc. [16,18–20], in nanomagnets. Furthermore, one can estimate the range of spin numbers S, where the crossover to classical superparamagnetic behavior of nanomagnets pertaining to a giant classical spin and that corresponding to the classical limit, $S \to \infty$, takes place (typically, this appears in the range $S \sim 20-50$ [14,17,19]). However, the results obtained in Refs. [13–20] using linear response theory cannot be applied to *nonlinear* phenomena such as the magnetization reversal in nanomagnets driven by a strong ac external magnetic field, nonlinear stochastic resonance, dynamic magnetic hysteresis (DMH), etc., because they automatically require the *nonlinear* ac stationary response in the presence of thermal agitation. Hitherto, that response for quantum nanomagnets has been determined via perturbation theory (e.g., Ref. [4]) by supposing that the potential energy of a spin in the external magnetic field is less than the thermal energy so that a small parameter exists. In the response to an ac field of *arbitrary strength*, however, such small parameters do not exist at all so that perturbation theory as used (implicitly) in the calculation of linear response characteristics (linear dynamic susceptibility, etc.) is now no longer applicable. However, as we shall now demonstrate, quantum effects in the nonlinear ac stationary response of nanomagnets with spin number $S \sim 10^0-10^4$ to an ac field of arbitrary strength can be determined by generalizing methods developed for classical spins [26] (see also [25], Chap. 9).

Here we shall demonstrate quantum effects in the nonlinear ac stationary response of the magnetization taking as an example a uniaxial paramagnet with arbitrary spin number S subjected to superimposed spatially *uniform* dc and ac fields

$\mathbf{H}_0$ and $\mathbf{H}(t) = \mathbf{H}\cos\omega t$, respectively, applied along the Z axis, i.e., the easy axis of magnetization. Thus, the time-dependent Hamiltonian $\hat{H}_S(t)$ has the axially symmetric form

$$\beta\hat{H}_S(t) = -\frac{\sigma}{S^2}\hat{S}_Z^2 - \frac{\xi_0 + \xi\cos\omega t}{S}\hat{S}_Z, \tag{1}$$

where $\hat{S}_Z$ is the operator associated with the Z component of the spin [24];σ is the dimensionless anisotropy constant; $\xi_0 = \beta S\hbar\gamma H_0$ and $\xi = \beta S\hbar\gamma H$ are the dc bias and ac field parameters, respectively; γ is the gyromagnetic ratio; $\hbar$ is Planck's constant; and $\beta = (kT)^{-1}$ is the inverse thermal energy. This Hamiltonian comprises a uniaxial anisotropy term $-\sigma\hat{S}_Z^2/S^2$ plus the Zeeman term $-(\xi_0 + \xi\cos\omega t)\hat{S}_Z/S$. In particular, it represents a generic model for spin-relaxation phenomena in molecular magnets, nanoclusters, etc. For large S, the Hamiltonian equation (1) describes the magnetization relaxation of classical superparamagnets such as magnetic nanoparticles [16]. Moreover, the time-independent Hamiltonian $-\sigma\hat{S}_Z^2/S^2 - \xi_0\hat{S}_Z/S$ is commonly used, e.g., to describe the magnetic properties of the dodecanuclear manganese molecular cluster Mn12 with $S = 10$, $\sigma T/S^2 = 0.6 - 0.7$ K [13,16]. In the standard basis of spin functions $|S,m\rangle$, which describe the states with definite spin S and spin projection m onto the Z axis, i.e., $\hat{S}_Z|S,m\rangle = m|S,m\rangle$, this Hamiltonian has an energy spectrum with a double-well structure and two minima at $m = \pm S$ separated by a potential barrier. Notice that in strong bias fields, $\xi_0 > \sigma(2S-1)/S$, the barrier disappears. Now generally speaking, spin reversal can take place either by thermal activation or by tunneling or a combination of both. The tunneling may occur from one side of the barrier to the other between resonant, equal-energy states coupled by transverse fields or high-order anisotropy terms [13,16]. The evolution equation for the reduced density matrix $\hat{\rho}$ describing the spin relaxation of a uniaxial paramagnet with the Hamiltonian $\hat{H}_S(t)$, Eq. (1), coupled to a thermal bath is

$$\frac{\partial\hat{\rho}(t)}{\partial t} + \frac{i}{\hbar}[\hat{H}_S(t),\hat{\rho}(t)] = \mathrm{St}\{\hat{\rho}(t)\}. \tag{2}$$

In Eq. (2), the collision kernel operator $\mathrm{St}\{\hat{\rho}(t)\}$ characterizing the spin-bath interaction we will employ is given by (see Appendix A)

$$\mathrm{St}\{\hat{\rho}(t)\} = \sum_{\mu=-1}^{1}(-1)^{\mu}D_{\mu}\{[\hat{S}_{\mu},\hat{\rho}(t)e^{\beta\hat{H}_S(t)/2}\hat{S}_{-\mu}e^{-\beta\hat{H}_S(t)/2}] + [e^{-\beta\hat{H}_S(t)/2}\hat{S}_{-\mu}e^{\beta\hat{H}_S(t)/2}\hat{\rho}(t),\hat{S}_{\mu}]\}. \tag{3}$$

Here the square brackets denote the commutators, viz., $[\hat{A},\hat{B}] = \hat{A}\hat{B} - \hat{B}\hat{A}$; D_{μ} are "diffusion" coefficients; $\hat{S}_0 = \hat{S}_Z$, $\hat{S}_{\pm1} = \mp(\hat{S}_X \pm i\hat{S}_Y)/\sqrt{2}$, and $\hat{S}_X$, $\hat{S}_Y$, $\hat{S}_Z$ are, respectively, the spherical and Cartesian components of the spin [27]. The above kinetic model was proposed by Hubbard [28] by generalizing Redfield's derivation [29] of the evolution equation for the reduced density matrix operator $\hat{\rho}$ to time-dependent Hamiltonians $\hat{H}_S(t)$ (the original Redfield derivation [29] was limited to time-independent Hamiltonians $\hat{H}_S$). As shown in Appendix A, the Hubbard model [28] of the collision kernel $\mathrm{St}\{\hat{\rho}(t)\}$ in the *short bath correlation time approximation*, can be simplified to yield Eq. (3) [22,30]. This simplification implies that the correlation time τ_c characterizing the thermal bath is short enough to approximate the stochastic process originating in the bath by a Markov process, thus qualitatively describing the spin relaxation in nanomagnets (at least in the high-temperature limit). In the parameter range, where the above approximation fails (e.g., throughout the very-low-temperature region), more general forms of the density matrix evolution equation must be used, e.g., those suggested in Refs. [13,14,16,17]. Using the above model, we will now calculate the nonlinear ac stationary response of a quantum uniaxial paramagnet with arbitrary S. Furthermore, we will show that our results in the weak ac field approximation, $\xi \ll 1$, coincide with existing linear response solutions [16,18] while in the classical limit, $S \to \infty$, they correspond with those of Ref. [26].

II. SOLUTION OF THE EVOLUTION EQUATION

For the Hamiltonian given by Eq. (1), the reduced density evolution Eq. (2) becomes

$$\begin{aligned}\frac{\partial\hat{\rho}}{\partial t} = {}& \frac{i}{\hbar\beta}\left\{\frac{\sigma}{S^2}[\hat{S}_0^2,\hat{\rho}] + \frac{\xi_0 + \xi\cos\omega t}{S}[\hat{S}_0,\hat{\rho}]\right\} \\ & + D_{\parallel}([\hat{S}_0,\hat{\rho}\hat{S}_0] + [\hat{S}_0\hat{\rho},\hat{S}_0]) \\ & - 2D_{\perp}\{e^{-\frac{\sigma}{2S^2} - \frac{\xi_0+\xi\cos\omega t}{2S}}[\hat{S}_{-1}e^{-\frac{\sigma}{S^2}\hat{S}_0}\hat{\rho},\hat{S}_{+1}] \\ & + e^{\frac{\sigma}{2S^2} + \frac{\xi_0+\xi\cos\omega t}{2S}}[\hat{S}_{+1}e^{\frac{\sigma}{S^2}\hat{S}_0}\hat{\rho},\hat{S}_{-1}]\},\end{aligned} \tag{4}$$

where we have introduced the notation $2D_{\perp} = D_{+1} = D_{-1}$ and $D_{\parallel} = D_0$ for the diffusion coefficients and have used the operator relations

$$\begin{aligned} & e^{\frac{\sigma}{2S^2}\hat{S}_0^2 + \frac{\xi_0+\xi\cos\omega t}{2S}\hat{S}_0}\hat{S}_{\pm1}e^{-\frac{\sigma}{2S^2}\hat{S}_0^2 - \frac{\xi_0+\xi\cos\omega t}{2S}\hat{S}_0} \\ & \quad = e^{-\frac{\sigma}{2S^2} \pm \frac{\xi_0+\xi\cos\omega t}{2S}}e^{\pm\frac{\sigma}{S^2}\hat{S}_0}\hat{S}_{\pm1}, \\ & \hat{S}_{\pm1}e^{\mp\frac{\sigma}{S^2}\hat{S}_0} = e^{\frac{\sigma}{S^2}}e^{\mp\frac{\sigma}{S^2}\hat{S}_0}\hat{S}_{\pm1}. \end{aligned}$$

Here the magnitude of the ac field ξ is supposed to be so large that the energy of a spin is either comparable to or higher than the thermal energy kT, i.e., $\xi \geqslant 1$, so that one is always faced with an intrinsically nonlinear problem which is solved as follows.

As far as the ac stationary response is concerned, use of the *symmetrized* collision kernel equation (4), is essential because only this form ensures the absence of the even harmonics in the magnetization nonlinear response for the symmetric uniaxial Hamiltonian $-\sigma\hat{S}_Z^2/S^2$. Now the crucial fact is that for *axially symmetric* Hamiltonians such as Eq. (1), the transformation of the evolution equation, Eq. (4), into differential-recurrence equations for its *individual* matrix elements may easily be accomplished because the diagonal entries of the density matrix then decouple from the nondiagonal ones. Hence, only the former contribute to the longitudinal spin relaxation allowing a complete solution. Consequently, we have from Eq. (4) the following three-term differential-recurrence equation for the *diagonal* entries $\rho_m = \rho_{mm}$:

$$\tau_N\frac{d\rho_m(t)}{dt} = q_m^-(t)\rho_{m-1}(t) + q_m(t)\rho_m(t) + q_m^+(t)\rho_{m+1}(t), \tag{5}$$

where $m=-S,-S+1,\ldots,S$, $\tau_N=(2D_\perp)^{-1}$ is the characteristic diffusion time and the time-dependent coefficients $q_m(t)$ and $q_m^{\pm}(t)$ are

$$q_m(t)=-a_m^- e^{-(2m-1)\frac{\sigma}{2S^2}-\frac{\xi_0+\xi\cos\omega t}{2S}}-a_m^+ e^{(2m+1)\frac{\sigma}{2S^2}+\frac{\xi_0+\xi\cos\omega t}{2S}},$$

$$q_m^{\pm}(t)=a_m^{\pm}e^{\mp(2m\pm1)\frac{\sigma}{2S^2}\mp\frac{\xi_0+\xi\cos\omega t}{2S}},$$

$$a_m^{\pm}=\frac{(S\mp m)(S\pm m+1)}{2}.$$

Now, our objective is to calculate the stationary ac response of the longitudinal component of the magnetization defined as

$$\langle\hat{S}_Z\rangle(t)=\sum_{m=-S}^{S} m\rho_m(t). \tag{6}$$

Since we are solely concerned with the ac response corresponding to the stationary state, which is independent of the initial conditions, we may seek the diagonal elements $\rho_m(t)$ as the Fourier series, viz.,

$$\rho_m(t)=\sum_{k=-\infty}^{\infty}\rho_m^k(\omega)e^{ik\omega t}. \tag{7}$$

As is evident from Eqs. (6) and (7), $\langle\hat{S}_Z\rangle(t)$ is then rendered as a Fourier series, viz.,

$$\langle\hat{S}_Z\rangle(t)=\sum_{k=-\infty}^{\infty}S_Z^k(\omega)e^{ik\omega t}, \tag{8}$$

where the amplitudes $S_Z^k(\omega)$ are themselves given by the finite series

$$S_Z^k(\omega)=\sum_{m=-S}^{S} m\rho_m^k(\omega). \tag{9}$$

Next, we recall the Fourier-Bessel expansion [31],

$$e^{\pm\frac{\xi}{2S}\cos\omega t}=\sum_{k=-\infty}^{\infty}I_k\left(\pm\frac{\xi}{2S}\right)e^{ik\omega t}, \tag{10}$$

where $I_k(z)$ are the modified Bessel functions of the first kind [31]. Thus by direct substitution of Eqs. (7) and (10) into Eq. (5), we have a recurrence relation in (k,m) between the Fourier coefficients $\rho_m^k(\omega)$, viz.,

$$\begin{aligned}ik\omega\tau_N\rho_m^k(\omega)=\sum_{k'=-\infty}^{\infty}\Bigg\{&a_m^- e^{\frac{\sigma(2m-1)}{2S^2}+\frac{\xi_0}{2S}}I_{k-k'}\left(\frac{\xi}{2S}\right)\rho_{m-1}^{k'}(\omega)+a_m^+ e^{-\frac{\sigma(2m+1)}{2S^2}-\frac{\xi_0}{2S}}I_{k-k'}\left(-\frac{\xi}{2S}\right)\rho_{m+1}^{k'}(\omega)\\&-\left[a_m^- e^{-\frac{\sigma(2m-1)}{2S^2}-\frac{\xi_0}{2S}}I_{k-k'}\left(-\frac{\xi}{2S}\right)+a_m^+ e^{\frac{\sigma(2m+1)}{2S^2}+\frac{\xi_0}{2S}}I_{k-k'}\left(\frac{\xi}{2S}\right)\right]\rho_m^{k'}(\omega)\Bigg\}.\end{aligned} \tag{11}$$

The recurrence relation Eq. (11) can be solved exactly for the Fourier amplitudes $\rho_m^k(\omega)$ via matrix continued fractions [25,32] (see Appendix B). Thus, having calculated $\rho_m^k(\omega)$, we have from Eq. (9) all the constituent Fourier amplitudes $S_Z^k(\omega)$ of the longitudinal component of the magnetization in Eq. (8).

III. LINEAR AND NONLINEAR DYNAMIC SUSCEPTIBILITIES

Initially, we treat the *frequency-dependent* fundamental component of the magnetization $S_Z^1(\omega)$. The simplest example is the linear response to a *vanishing ac field*; i.e., when the ac field parameter $\xi\to 0$, then the normalized fundamental component $S_Z^1(\omega)/S_Z^1(0)$ of the Fourier series, Eq. (8), which is all that is ever needed for the linear response, will yield the normalized *linear* dynamic susceptibility, viz.,

$$\frac{\chi(\omega)}{\chi}=\frac{S_Z^1(\omega)}{S_Z^1(0)}, \tag{12}$$

where χ is the static susceptibility defined as

$$\begin{aligned}\chi&=\left\langle\hat{S}_Z^2\right\rangle_0-\langle\hat{S}_Z\rangle_0^2\\&=\sum_{m=-S}^{S}m^2\rho_m^0-\left(\sum_{m=-S}^{S}m\rho_m^0\right)^2,\end{aligned}$$

with the matrix elements

$$\rho_m^0=\frac{1}{Z_S}e^{\sigma m^2/S^2+\xi_0 m/S},$$

and the partition function Z_S given by

$$Z_S=\sum_{m=-S}^{S}e^{\sigma m^2/S^2+\xi_0 m/S}. \tag{13}$$

However, the longitudinal linear dynamic susceptibility $\chi(\omega)$ can also be obtained via the Kubo relation [25,30]

$$\frac{\chi(\omega)}{\chi}=1-i\omega\tilde{C}(\omega), \tag{14}$$

where $\tilde{C}(\omega)=\int_0^\infty C(t)e^{-i\omega t}dt$ is the one-sided Fourier transform of the normalized longitudinal equilibrium correlation function $C(t)$ given by

$$C(t)=\frac{1}{\beta\chi}\left\langle\int_0^\beta[\hat{S}_Z(-i\lambda\hbar)-\langle\hat{S}_Z\rangle_0][\hat{S}_Z(t)-\langle\hat{S}_Z\rangle_0]d\lambda\right\rangle.$$

The normalized longitudinal equilibrium correlation function $C(t)$ describes the *linear response* of a uniaxial paramagnet to *infinitesimally small* changes in the magnitude of the dc field $\mathbf{H}_0$ alone. In determining this response, it is supposed that the uniform dc field $\mathbf{H}_0$ is directed along the Z axis of the laboratory coordinate system and that a *small* probing field $\mathbf{H}$ having been applied to the assembly of noninteracting spins in the distant past ($t=-\infty$) so that equilibrium conditions obtain at time $t=0$, is suddenly switched off at $t=0$. In the low- ($\omega\to 0$) and high- ($\omega\to\infty$) frequency limits, we have

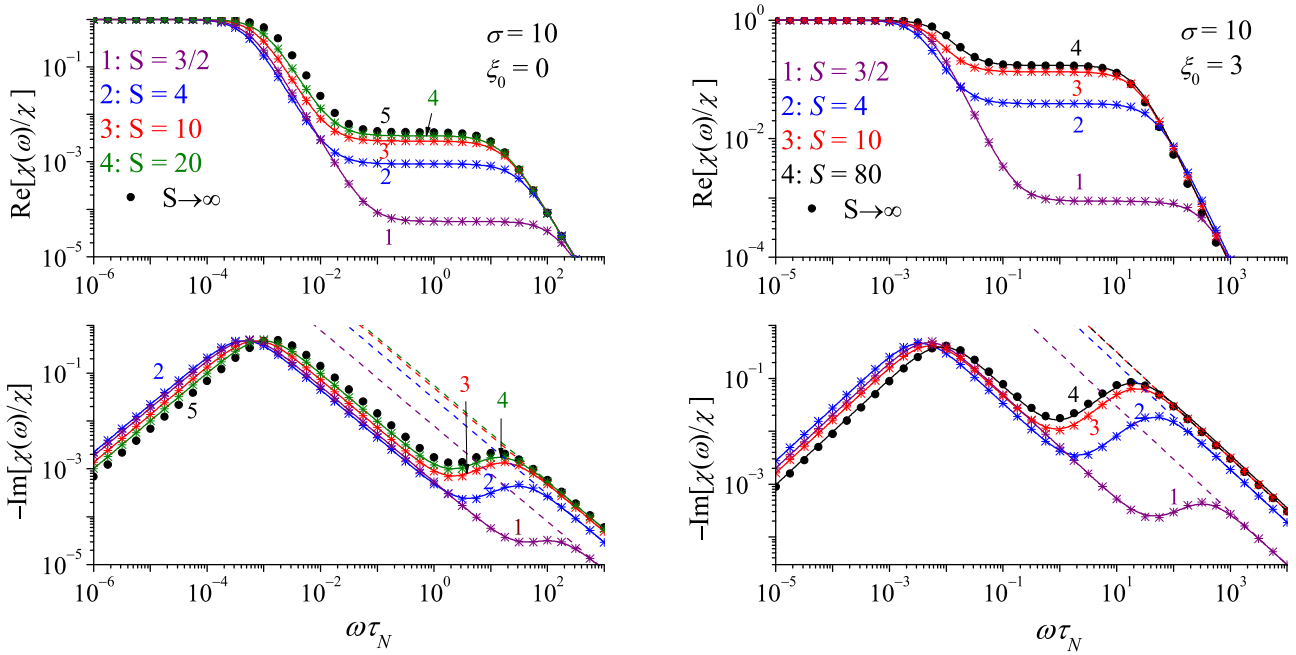

FIG. 1. (Color online) The normalized linear susceptibility $\chi(\omega)/\chi$, Eq. (12), vs normalized frequency $\omega\tau_N$ for the anisotropy parameter $\sigma = 10$, the uniform field parameter (a) $\xi_0 = 0$ and (b) $\xi_0 = 3$, and various spin numbers S. Asterisks: the two-mode approximation, Eq. (22). Dashed lines: the high-frequency asymptote, from Eqs. (16) and (18). Filled circles: the classical limit $S \to \infty$.

from Eq. (14)

$$\chi(\omega) \approx \chi(1 - i\omega\tau_{\rm cor} + \cdots), \quad \omega \to 0, \tag{15}$$

$$\chi(\omega) \sim \chi(i\omega\tau_{\rm ef})^{-1} + \cdots, \quad \omega \to \infty, \tag{16}$$

where

$$\tau_{\rm cor} = \int_0^\infty C(t)dt \quad \text{and} \quad \tau_{\rm ef} = -\frac{C(0)}{\dot{C}(0)},$$

are, respectively, the integral and effective relaxation times given by [16,18]

$$\tau_{\rm cor} = \frac{2\tau_N}{\chi} \sum_{k=1-S}^{S} \frac{\left[\sum_{m=k}^{S}(m - \langle\hat{S}_Z\rangle_0)\rho_m^0\right]^2}{[S(S+1) - k(k-1)]\sqrt{\rho_k^0\rho_{k-1}^0}}, \tag{17}$$

$$\tau_{\rm ef} = \frac{2\chi\tau_N}{\sum_{k=1-S}^{S}[S(S+1) - k(k-1)]\sqrt{\rho_k^0\rho_{k-1}^0}}. \tag{18}$$

We remark that the linear response has been previously studied by Garanin [13] and García-Palacios and Zueco [16] thereby yielding analytic expressions including the characteristic relaxation times $\tau_{\rm cor}$, $\tau_{\rm ef}$, and $\tau \approx \lambda_1^{-1}$ even for more general models of spin-bath interactions than we have used here. Garanin's method yields for the model at hand

$$\tau = \frac{2\tau_N}{\chi_\Delta} \sum_{k=-S}^{S-1} \times \frac{\left[\sum_{m=-S}^{k}(m - \langle\hat{S}_Z\rangle_0)\rho_m^0\right]\left\{\sum_{m=-S}^{k}[\mathrm{sgn}(m-m_b) - \Delta]\rho_m^0\right\}}{[S(S+1) - k(k+1)]\sqrt{\rho_k^0\rho_{k+1}^0}}, \tag{19}$$

where m_b is the quantum number corresponding to the top of the barrier, with

$$\Delta = \sum_{m=-S}^{S} \mathrm{sgn}(m - m_b)\rho_m^0$$

and

$$\chi_\Delta = \sum_{m=-S}^{S} m\,\mathrm{sgn}(m - m_b)\rho_m^0 - \left(\sum_{m=-S}^{S} m\rho_m^0\right)\left[\sum_{m=-S}^{S} \mathrm{sgn}(m - m_b)\rho_m^0\right].$$

In Fig. 1, we plot the real and imaginary parts of the linear dynamic susceptibility $\chi(\omega)/\chi$ as calculated from the matrix continued fraction solution, rendered in the form of Eqs. (9) and (12) for zero dc field, $\xi_0 = 0$ (symmetrical wells) and for nonzero dc field, $\xi_0 = 3$ (asymmetrical wells). Two distinct bands appear in the magnetic loss spectrum $-\mathrm{Im}[\chi(\omega)]$. The low-frequency band is due to the "overbarrier" relaxation mode

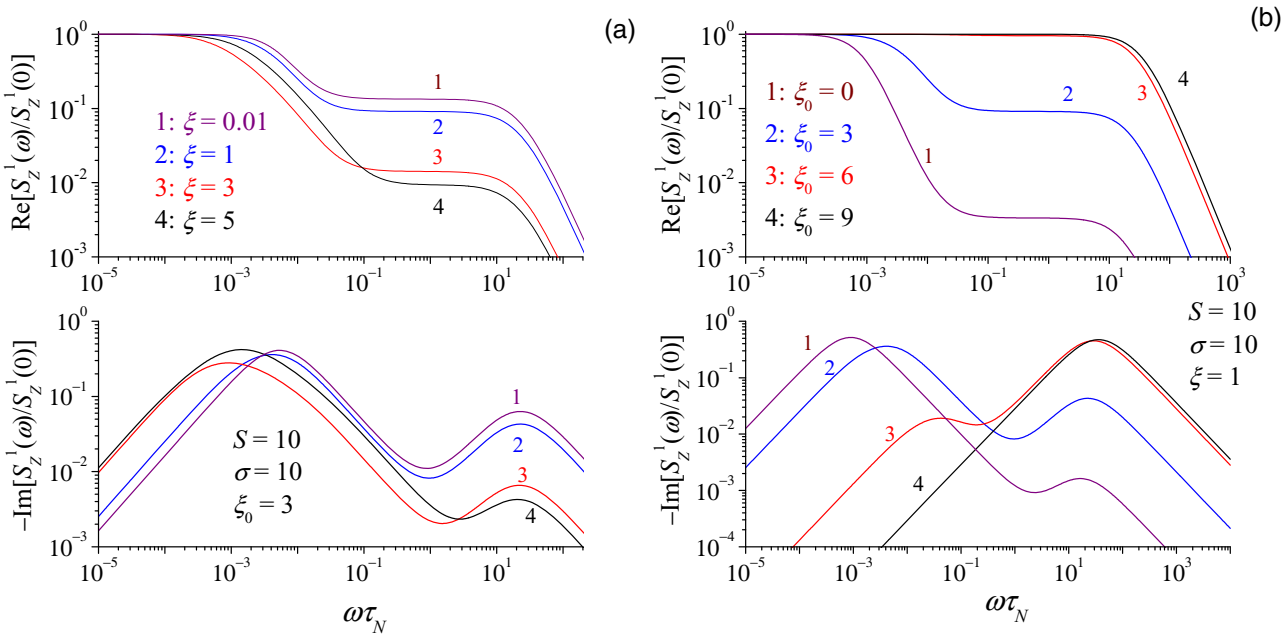

FIG. 2. (Color online) The real and imaginary parts of the normalized fundamental component $S_Z^1(\omega)/S_Z^1(0)$ vs normalized frequency $\omega\tau_N$ (a) for various values of the applied ac stimulus $\xi = 0.01$ (linear response), 1, 3, 5, and the dc field parameter $\xi_0 = 3$, and (b) for various dc field parameters ξ_0 and $\xi = 1$; the spin number $S = 10$ and anisotropy parameter $\sigma = 10$.

and can be described by a *single* Lorentzian, namely,

$$\frac{\chi(\omega)}{\chi} \approx 1 - \frac{i\omega\tau_{\rm cor}}{1 + i\omega\tau}, \tag{20}$$

where τ is the longest relaxation time, which may be identified with the spin reversal time, and is calculated via the inverse of the smallest *nonvanishing* eigenvalue λ_1 of the system matrix equation (C1) from Appendix C. Now τ must also be related to the frequency $\omega_{\rm max}$ of the low-frequency peak in the magnetic loss spectrum $-{\rm Im}[\chi(\omega)]$, where it attains a maximum, and/or the half width $\Delta\omega$ of the spectrum of the real part of the susceptibility ${\rm Re}[\chi(\omega)]$ via

$$\tau \approx \omega_{\rm max}^{-1} \approx \Delta\omega^{-1}. \tag{21}$$

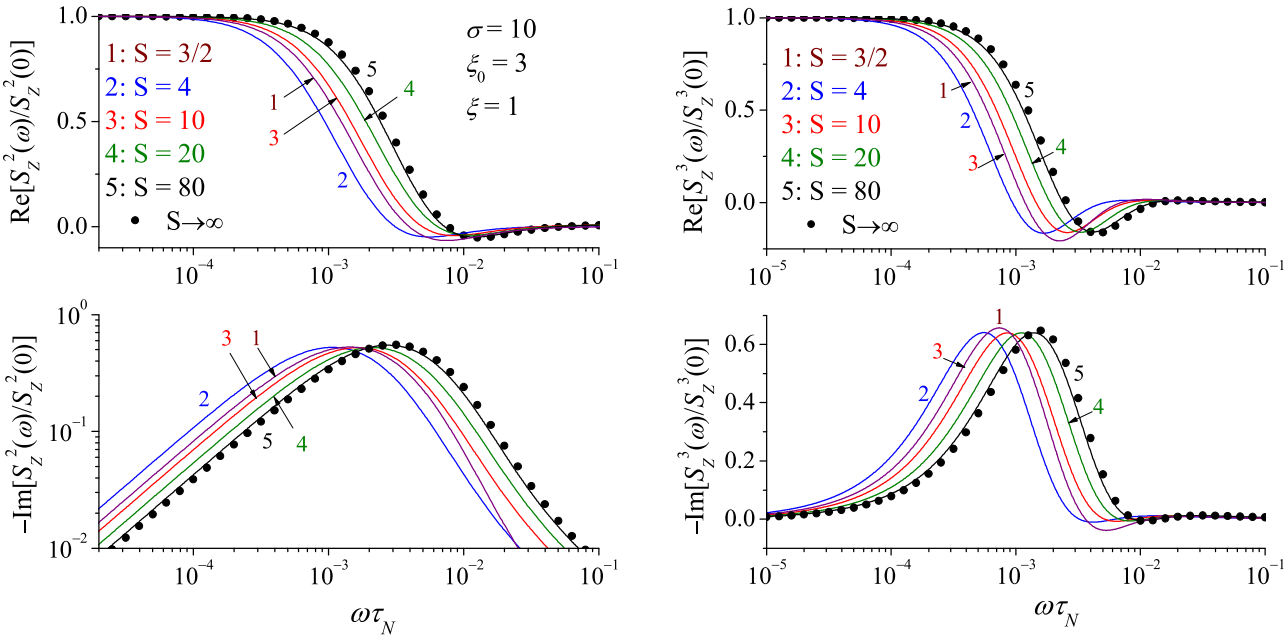

FIG. 3. (Color online) The real and imaginary parts of the normalized second- and third-harmonic components $S_Z^2(\omega)/S_Z^2(0)$ and $S_Z^3(\omega)/S_Z^3(0)$ of the nonlinear response vs $\omega\tau_N$ for anisotropy parameter $\sigma = 10$, the dc field parameter $\xi_0 = 3$, the ac field parameter $\xi = 1$, and various spin numbers S. Filled circles: the classical limit.

Regarding the second high-frequency band, this is due to high-frequency individual "intrawell" modes [16,22], which are virtually indistinguishable in the spectrum of $\chi''(\omega)$ appearing merely as a single high-frequency Lorentzian band. Thus, we may describe the behavior of $\chi(\omega)/\chi$ via a two-mode approximation, i.e., by supposing that it is given as a sum of two Lorentzians, viz. [16,22,25,33],

$$\frac{\chi(\omega)}{\chi} \approx \frac{1-\delta}{1+i\omega\tau} + \frac{\delta}{1+i\omega\tau_W}. \tag{22}$$

Here τ_W is a characteristic relaxation time of the near-degenerate high-frequency well modes and δ denotes a parameter characterizing their contribution to the susceptibility defined as

$$\delta = \frac{\frac{\tau_{\rm cor}}{\tau} + \frac{\tau}{\tau_{\rm ef}} - \frac{\tau_{\rm cor}}{\tau_{\rm ef}} - 1}{\frac{\tau_{\rm cor}}{\tau} + \frac{\tau}{\tau_{\rm ef}} - 2}, \quad \tau_W = \frac{\tau_{\rm cor} - \tau}{1 - \frac{\tau}{\tau_{\rm ef}}}. \tag{23}$$

The parameters δ and τ_W in Eqs. (22) and (23) have been determined by imposing the condition that the approximate two-mode equation (22) must obey the *exact* asymptotic equations (15) and (16). In order to verify this analytical description of the quantum behavior, we compare it in Fig. 1 with the real and imaginary parts of $\chi(\omega)/\chi$ as calculated from the exact numerical solutions. It is apparent from Fig. 1 that at low frequencies no *practical difference exists between the numerical solution and the two-mode approximation* (the maximum relative deviation between the corresponding curves does not exceed a few percent). In the classical limit, $S \to \infty$, the axially symmetric Hamiltonian defined by Eq. (1) corresponds to a normalized free energy V given by

$$\beta V(\vartheta) = -\sigma\cos^2\vartheta - \xi_0\cos\vartheta. \tag{24}$$

This classical limit is also shown in Fig. 1 for comparison. Our conclusions mirror those of García-Palacios and Zueco [16] who have also shown that the two-mode approximation, which was originally developed for classical systems [33], accurately describes the *linear* response of quantum paramagnets.

Turning our attention to the nonlinear response, where all terms in k in Eq. (10) must now be included, we see that in *strong* ac fields, pronounced nonlinear effects occur as the amplitude of the field increases (see Figs. 2 and 3). As in the linear response, two distinct absorption bands again appear in the spectrum of the imaginary part of the fundamental, viz.,$-\mathrm{Im}[S_Z^1(\omega)/S_Z^1(0)]$. Thus, two corresponding dispersion regions occur in the spectrum of $\mathrm{Re}[S_Z^1(\omega)/S_Z^1(0)]$. However, due to the pronounced nonlinear effects (see Fig. 2) the low-frequency band of $-\mathrm{Im}[S_Z^1(\omega)/S_Z^1(0)]$ now deviates from the Lorentzian shape so that it may no longer be approximated by a *single* Lorentzian. Nevertheless, the frequency of maximum absorption as defined in Eq. (21) may still be used to estimate an effective reversal time τ as $\tau \approx \Delta\omega^{-1}$. The behavior of the low-frequency peak of $-\mathrm{Im}[S_Z^1(\omega)/S_Z^1(0)]$ as *a function of the ac field amplitude* crucially depends on whether or not a dc field is applied. For strong dc bias, $\xi_0 > 1$ (see Fig. 2), the low-frequency peak shifts to lower frequencies reaching a maximum at $\xi \sim \xi_0$, thereafter shifting to higher frequencies with increasing ξ_0. In other words, as the dc field increases, the reversal time of the spin *initially increases* and having attained its maximum at some critical value $\xi \sim \xi_0$, thereafter decreases. This behavior agrees with that observed in the classical case [16,33]. The fundamental component $S_Z^1(\omega)/S_Z^1(0)$, which in principle now depends on all the other frequency components, is also shown in Fig. 2 for various dc field parameters ξ_0. Also for zero dc bias, $\xi_0 = 0$, the low-frequency peak shifts to higher frequencies with increasing ξ.

Now, a striking feature of the nonlinear response is that the effective reversal time may also be evaluated from either the spectrum of the (now) frequency-dependent dc component $S_Z^0(\omega)$ (for nonzero dc bias, $\xi_0 \neq 0$) or those of the higher-order harmonics $S_Z^k(\omega)$ with $k > 1$ because the low-frequency parts of these spectra are themselves, like the spectra of the fundamental, dominated by overbarrier relaxation processes. For illustration, the real and imaginary parts of the normalized second- and third-harmonic components $S_Z^2(\omega)/S_Z^2(0)$ and $S_Z^3(\omega)/S_Z^3(0)$ of the response are shown in Fig. 3. Like the fundamental, the behavior of both $-\mathrm{Im}[S_Z^2(\omega)/S_Z^2(0)]$ and $-\mathrm{Im}[S_Z^3(\omega)/S_Z^3(0)]$ depends on whether or not a dc field is applied. For *weak* dc bias field $\xi_0 < 0.5$, the low-frequency peak shifts monotonically to higher frequencies. For *strong* dc

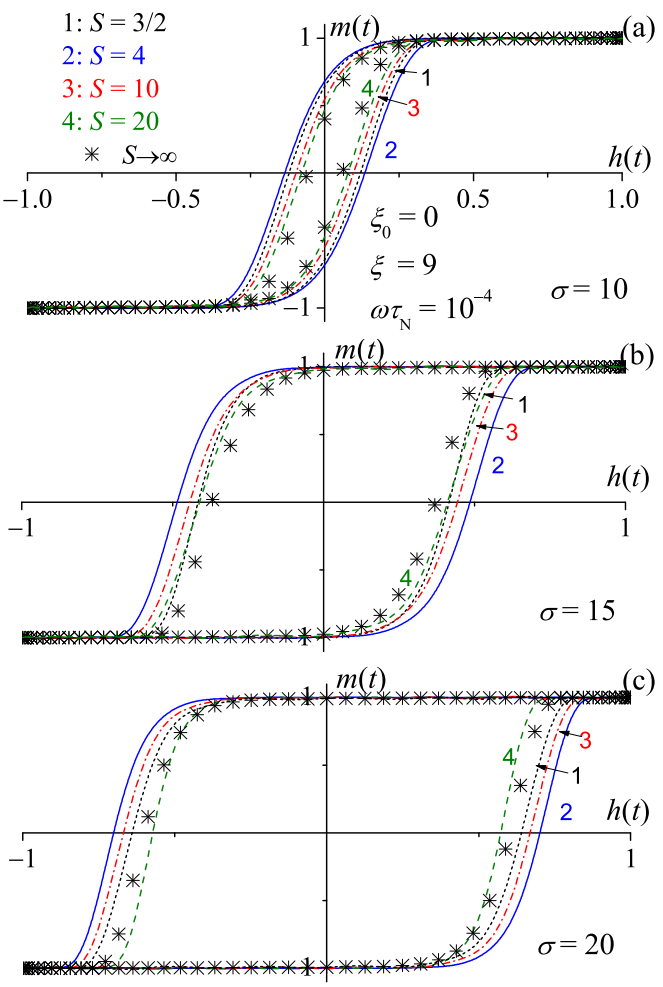

FIG. 4. (Color online) DMH loops $[m(t) = \langle\hat{S}_Z\rangle(t)/S$ vs $h(t) = \cos\omega t]$ for various anisotropy parameters $\sigma = 10$ (a), 15 (b), 20 (c), and various spin numbers $S = 3/2$ (1: short-dashed lines), 4 (2: solid lines), 10 (3: dashed-dotted lines), 20 (4: dashed lines), and ∞ (asterisks) at $\omega\tau_N = 10^{-4}$, $\xi_0 = 0$, and $\xi = 9$.

bias field, $\xi_0 > 1$, on the other hand, the low-frequency peak shifts to lower frequencies reaching a maximum at $\xi \sim \xi_0$, thereafter decreasing with increasing ξ.

IV. DYNAMIC MAGNETIC HYSTERESIS

Studies of DMH in magnetic nanoparticles subjected to thermal fluctuations having been initiated by Ignatchenko and Gekht [9] were later extended in many other investigations (see, e.g., Refs. [10–12]). Like the classical case, DMH loops for quantum nanomagnets represent a parametric plot of the steady-state time-dependent normalized magnetization as a function of the applied ac field, i.e.,

$$m(t) = \langle \hat{S}_Z \rangle(t)/S \quad \text{vs} \quad h(t) = H(t)/H = \cos \omega t.$$

Thus, we can calculate the normalized area of the DMH loop A_n defined as

$$A_n = \frac{1}{4} \oint m(t) dh(t) = -\frac{\pi}{2S} \mathrm{Im}\big[S_Z^1(\omega)\big], \qquad (25)$$

which is the energy loss per particle over one cycle of the ac field.

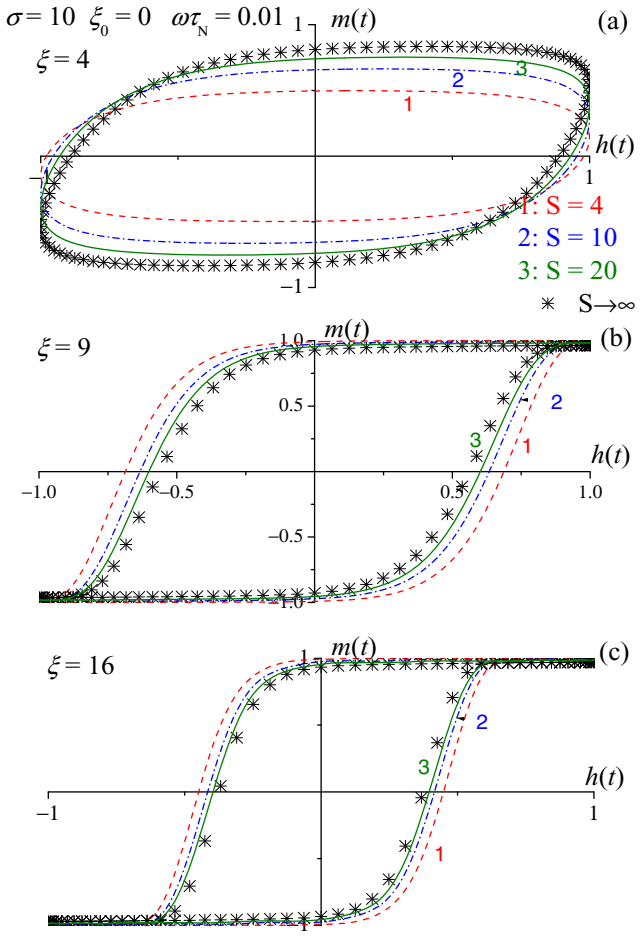

FIG. 5. (Color online) DMH loops for various ac external field parameters $\xi = 4$ (a), 9 (b), 16 (c), and various spin numbers $S = 4$ (1: dashed lines), 10 (2: dashed-dotted lines), 20 (3: solid lines), and ∞ (asterisks) at $\sigma = 10$, $\xi_0 = 0$, and $\omega\tau_N = 10^{-2}$.

In Figs. 4–7 we show the effects of ac and dc bias magnetic fields on the DMH loops in a uniaxial nanomagnet with arbitrary S. For a *weak* ac field, $\xi \to 0$, the DMH loops are [cf. Eq. (26) below] ellipses with normalized area A_n given by Eq. (25); the behavior of $A_n \sim -\mathrm{Im}[S_Z^1(\omega)]$ being similar [cf. Eq. (25)] to that of the magnetic loss $\chi''(\omega)$ (see Fig. 1). The susceptibility given by the two-mode equation (22) implies that the overall relaxation process consists of two distinct entities, namely, the slow thermally activated (overbarrier or interwell) process and the fast (intrawell) relaxation in the wells. Now, at low frequencies and for large barriers between the wells, only the first term on the right side in Eq. (22) for $\mathrm{Im}[S_Z^1(\omega)]$ need be considered. Furthermore, for *weak* dc bias fields, $\xi_0/(2\sigma) \ll 1$, the approximation $\delta \approx 1$ may also be used so that the *normalized* magnetization $m(t) = \langle \hat{S}_Z \rangle(t)/S$ is given by the simple (linear response) formula [14],

$$m(t) = \frac{1}{S}\langle \hat{S}_Z \rangle_0 + \frac{\chi \xi}{S} \frac{\cos \omega t + \omega\tau \sin \omega t}{1 + \omega^2 \tau^2}, \qquad (26)$$

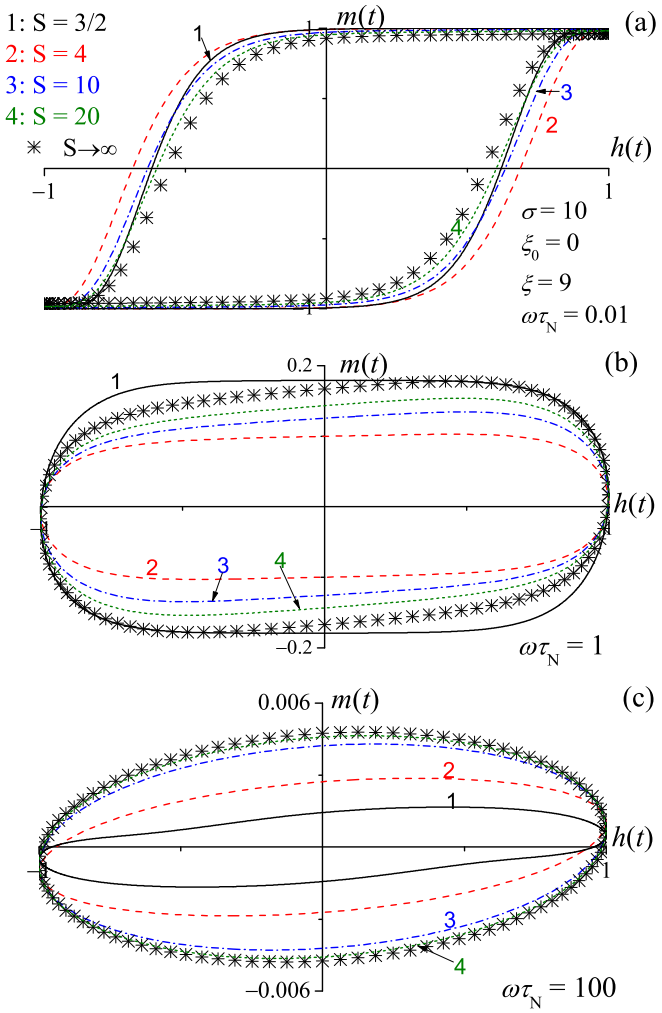

FIG. 6. (Color online) DMH loops for various dimensionless frequencies $\omega\tau_N = 10^{-2}$ (a), 1 (b), 10^2 (c), and various spin numbers $S = 3/2$ (1: solid lines), 4 (2: dashed lines), 10 (3: dashed-dotted lines), 20 (4: short-dashed lines), and ∞ (asterisks) at $\sigma = 10$, $\xi_0 = 0$, and $\xi = 9$.

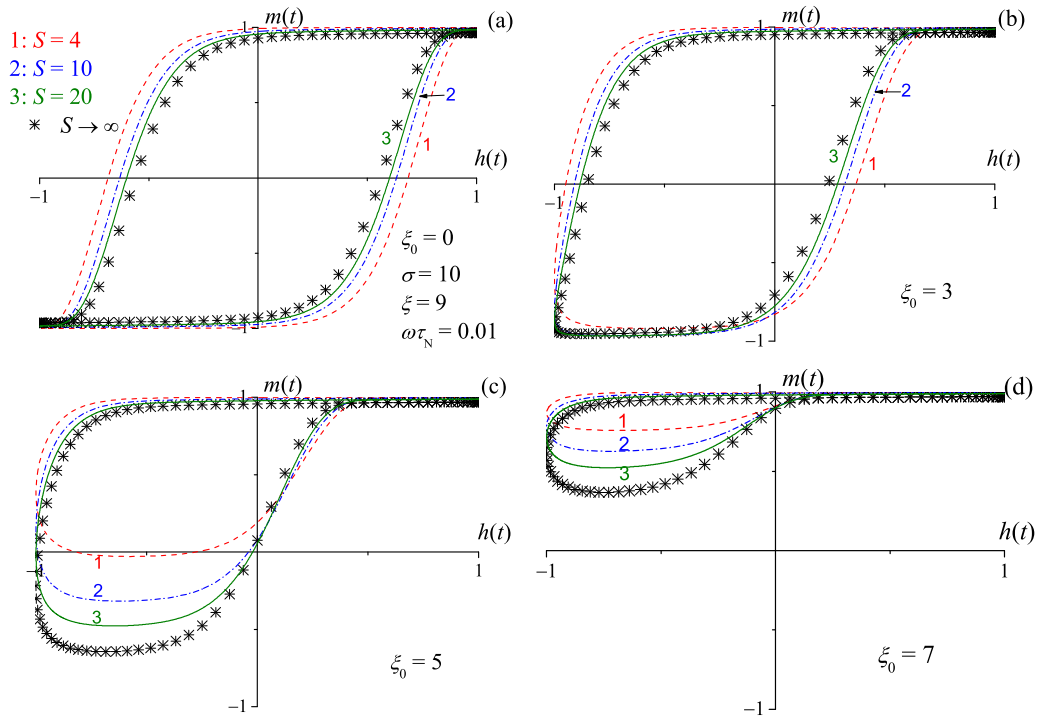

FIG. 7. (Color online) DMH loops for various constant field parameters $\xi_0 = 0$ (a), 3 (b), 5 (c), 7 (d), and various spin numbers $S = 4$ (1: dashed lines), 10 (2: dashed-dotted lines), 20 (3: solid lines), and ∞ (asterisks) at $\xi = 9$, $\sigma = 10$, and $\omega\tau_N = 10^{-2}$.

with $\tau = \lambda_1^{-1}$ and μ is the magnetic moment. If we introduce the normalizations

$$x(t) = \cos\omega t \quad \text{and} \quad y(t) = \frac{Sm(t) - \langle \hat{S}_z \rangle_0}{\chi\xi},$$

and eliminate the time between these two equations, we then have the Cartesian equation of an ellipse in the (x, y) plane, namely, [12b],

$$x^2 + \frac{1}{\omega^2\tau^2}[(1 + \omega^2\tau^2)y - x]^2 = 1. \tag{27}$$

For *moderate* ac fields corresponding to $\xi \approx 1$, although an analytical formula for $m(t)$ is now unavailable, nevertheless, the DMH loops still have approximately an ellipsoidal shape implying that only a few harmonics actually contribute to the weakly nonlinear response. In contrast in *strong* ac fields, $\xi > 1$, the shape alters substantially and so the normalized area A_n now exhibits a pronounced dependence on the frequency ω, and the ac and dc bias field amplitudes ξ and ξ_0, as well as on the anisotropy parameter σ and the spin number S (see Figs. 4–7). In this regime, the external ac field is able to saturate the paramagnetic moment as well as to induce its inversion (i.e., switching between the directions of the easy axis). In Figs. 4 and 5, we plot the loops for various S and anisotropy (σ) and ac field (ξ) parameters exemplifying how their shapes (and consequently their areas) alter as these parameters vary. Clearly, the remagnetization time is highly sensitive to variations of these parameters. For example, with a strong ac driving field, the Arrhenius dependence of the reversal time on temperature $\log(\tau) \propto 1/T$, which accurately accounts for the linear response regime, is modified because the strong ac field intervenes so drastically reducing the effective response time of the paramagnet. Thus, the nonlinear behavior facilitates remagnetization regimes, which are never attainable with weak ac fields—the reason being that the dc bias component under the appropriate conditions *efficiently tunes* this effect by either *enhancing* or *blocking* the action of the strong ac field. The *pronounced* frequency dependence of the loops is highlighted in Fig. 6 for various S. At low frequencies, the field changes are *quasiadiabatic*, so that the magnetization reverses due to the *cooperative* shuttling action of thermal agitation combined with the ac field. The dc bias field effects on the DMH are illustrated in Fig. 7 showing the changes in the DMH caused by varying ξ_0 for various spin numbers S. In order to understand the effect of the dc bias field on the loop area, one must first recall that the magnetic relaxation time depends on the actual value of the applied field. Under the conditions of Fig. 7, the *positive limiting* (saturation) value of $m(t) \to 1$ corresponds to a total field $H_0 + H$, thus *favoring* the magnetization relaxation to the positive saturation value $m(t) \to 1$. However, for *negative* $h(t)$, the total field $H_0 - H$ is much weaker and so cannot induce relaxation to the negative saturation value $m(t) \to -1$. Therefore, the "center of area" of the loop moves upwards. In the classical limit, $S \to \infty$, our results concur with those for classical uniaxial nanomagnets [11,12].

The temperature dependence of the DMH is governed by the dimensionless anisotropy (inverse temperature) parameter $\sigma \propto 1/T$. The normalized DMH area A_n as a function of σ^{-1} is shown in Fig. 8 for various S showing that the tuning action of the dc bias field described above is effective over a certain temperature interval. This conclusion once again indicates that

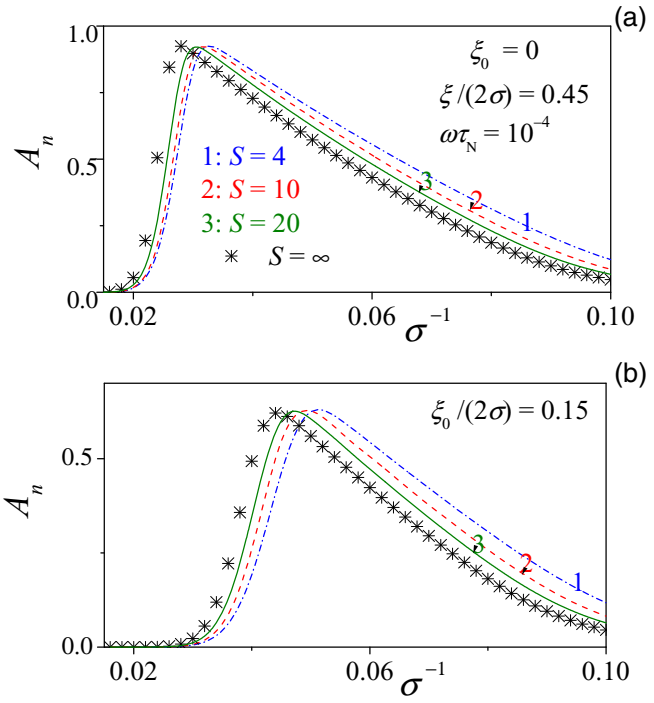

FIG. 8. (Color online) Normalized area of the DMH loop A_n vs the dimensionless temperature σ^{-1} under variation of the dc bias field parameter $h_0 = \xi_0/(2\sigma) = 0$ (a) and 0.15 (b) for various spin numbers $S = 4$ (dashed-dotted lines), 10 (dashed lines), 20 (solid lines), and ∞ (asterisks) at the frequency $\omega\tau_N = 10^{-4}$ and the ac field amplitude $\xi/(2\sigma) = 0.45$.

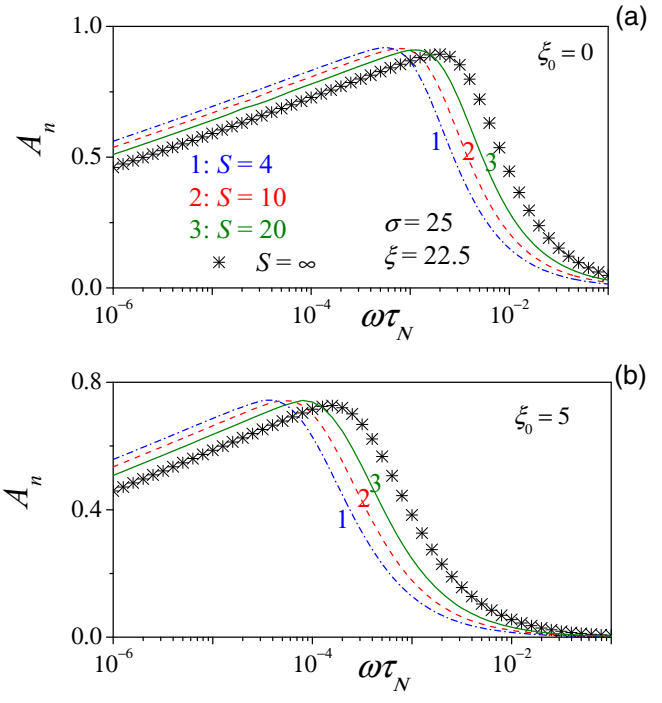

FIG. 9. (Color online) Normalized area of the DMH loop A_n vs the dimensionless frequency $\omega\tau_N$ under variation of the dc bias field $\xi_0 = 0$ (a) and 5 (b) for various spin numbers $S = 4$ (dashed-dotted lines), 10 (dashed lines), 20 (solid lines), and ∞ (asterisks). The anisotropy parameter $\sigma = 25$ and the ac field parameter $\xi/(2\sigma) = 0.45$.

the relaxation of the magnetization is mostly caused by thermal fluctuations, implying that the magnetic response time retains a strong temperature dependence. The normalized area as a function of the frequency ω and ac field parameter $\xi/(2\sigma)$ is shown in Figs. 9 and 10, respectively. Clearly A_n can invariably be represented as a nonmonotonic curve with a maximum the position of which is determined by S as well as by the other model parameters. The peak in A_n (Fig. 9) is caused by the field-induced modifications of the reversal time as strongly tuned by the dc bias field. As in Fig. 9, variation of the dc field strength shifts the frequency, where the maximum is attained, by several orders of magnitude. The normalized loop area presented in Fig. 10 illustrates the dependence of A_n on the ac field amplitude, which is similar to that of classical superparamagnets.

V. CONCLUSIONS

We have studied the nonlinear ac stationary response of uniaxial paramagnets with arbitrary spin number S subjected to superimposed ac and dc magnetic fields in the high-temperature and weak spin-bath coupling limit. The nonlinear dynamic susceptibility and DMH in such nanomagnets has been treated without any *a priori* assumptions regarding the magnetizing field strength and the spin number S. In general, it appears that given appropriate conditions a small (in comparison with the internal anisotropy field) bias dc field can profoundly affect the nonlinear dynamic susceptibility and shape of the DMH loops in nanomagnets accompanied by a

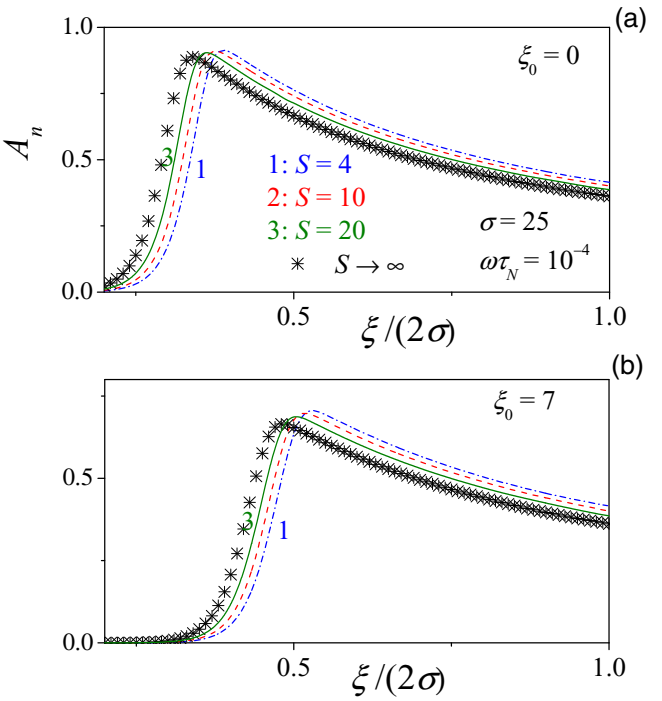

FIG. 10. (Color online) Normalized area of the DMH loop A_n vs the ac field amplitude $\xi/(2\sigma)$ under variation of the bias field parameter $\xi_0 = 0$ (a), 2.5 (b), 5 (c), and 7 (d) for various spin numbers $S = 4$ (dashed-dotted lines), 10 (dashed lines), 20 (solid lines), and ∞ (asterisks). The anisotropy parameter $\sigma = 25$ and frequency $\omega\tau_N = 10^{-4}$.

strong dependence on S. The overall conclusion is that just as in linear response [16,19], one may determine the transition from quantum elementary spin relaxation to that pertaining to a giant spin as a function of the spin number S yielding explicitly the evolution of the nonlinear ac stationary response and DMH from that of molecular magnets ($S \sim 10$) to nanoclusters ($S \sim 100$), and to classical superparamagnets. In the large spin limit, the solutions obtained via the evolution equation for the density matrix reduce to those yielded by the Fokker-Planck equation for the orientation distribution function of classical spins [25,26], while for linear response, the results entirely agree with those given in Ref. [19]. Hence, the results indicate that quantum effects in the nonlinear spin relaxation can be treated in a manner linking directly to the classical representations. Here we have only considered the nonlinear dynamic susceptibility and DMH of uniaxial paramagnets in the simplest configuration, i.e., where the ac and dc magnetic fields are applied along the easy axis of the nanomagnet. The calculation may, in principle, be generalized to other interesting cases such as arbitrary directions of applied fields and nonaxially symmetric anisotropies (cubic, biaxial, etc.).

ACKNOWLEDGMENTS

This publication has emanated from research conducted with the financial support of FP7-PEOPLE-Marie Curie Actions—International Research Staff Exchange Scheme (Project No. PIRSES-GA-2011-295196 - DMH).

APPENDIX A: COLLISION KERNEL FOR THE TIME-DEPENDENT HAMILTONIAN IN THE HIGH-TEMPERATURE LIMIT

To derive Eq. (3), we follow Hubbard [28] who considered the general case of the time-dependent Hamiltonian $\hat{H}_S = \hat{H}_S(t)$. The collision kernel used by Hubbard is (in our notation)

$$\begin{aligned}\mathrm{St}(\hat{\rho}) = \sum_{\mu=-1}^{1}\sum_{r}(-1)^{\mu}e^{i\omega_r^{-\mu}t}D_{\mu}\left(\omega_r^{-\mu}\right)\\ \times\left\{e^{\beta\hbar\omega_r^{-\mu}/2}\left[\hat{S}_{\mu},\hat{\rho}\hat{U}^{-1}(t)\hat{S}^{r}_{-\mu}\hat{U}(t)\right]\right.\\ \left.+e^{-\beta\hbar\omega_r^{-\mu}/2}\left[\hat{U}^{-1}(t)\hat{S}^{r}_{-\mu}\hat{U}(t)\hat{\rho},\hat{S}_{\mu}\right]\right\},\end{aligned} \tag{A1}$$

where $\hat{S}^{r}_{\mu'}$ are the coefficients in the series expansion of the time-dependent spin operators $\hat{S}_{\mu'}(t) = \hat{U}(t)\hat{S}_{\mu'}\hat{U}^{-1}(t)$, namely,

$$\hat{S}_{\mu'}(t) = \sum\nolimits_{r}\hat{S}^{r}_{\mu'}e^{i\omega_r^{\mu'}t}, \tag{A2}$$

where $\omega_r^{\mu'}$ represents a parameter, while the operator $\hat{U}(t)$ is defined as

$$\hat{U}(t) = e^{\frac{i}{\hbar}\int_0^t \hat{H}_S(t')dt'}, \tag{A3}$$

and $D_{\mu}(\omega)$ is the correlation function of the bath written in the frequency domain as

$$D_{\mu} = \tilde{C}^{sym}_{\mu}(\omega)\mathrm{sech}(\beta\hbar\omega/2), \tag{A4}$$

with the symmetrized spectral density $\tilde{C}^{sym}_{\mu}(\omega) = [\tilde{C}_{\mu,-\mu}(-\omega) + \tilde{C}^{*}_{\mu,-\mu}(\omega)]/2$ which determines the spectrum of the *symmetrized* bath correlation functions. Then by reconverting the result to operator form [see Eq. (A2)], we have for the collision kernel

$$\begin{aligned}\mathrm{St}(\hat{\rho}) &= \sum_{\mu=-1}^{1}\sum_{r}(-1)^{\mu}D_{\mu}e^{i\omega_r^{-\mu}t}\left\{e^{\beta\hbar\omega_r^{-\mu}/2}\left[\hat{S}_{\mu},\hat{\rho}\hat{U}^{-1}(t)\hat{S}^{r}_{-\mu}\hat{U}(t)\right] + e^{-\beta\hbar\omega_r^{-\mu}/2}\left[\hat{U}^{-1}(t)\hat{S}^{r}_{-\mu}\hat{U}(t)\hat{\rho},\hat{S}_{\mu}\right]\right\}\\ &= \sum_{\mu=-1}^{1}(-1)^{\mu}D_{\mu}\left\{\left[\hat{S}_{\mu},\hat{\rho}\hat{U}^{-1}(t)\hat{U}(t-i\beta\hbar/2)\hat{S}_{-\mu}\hat{U}^{-1}(t-i\beta\hbar/2)U(t)\right]\right.\\ &\quad\left.+\left[\hat{U}^{-1}(t)\hat{U}(t+i\beta\hbar/2)\hat{S}_{-\mu}\hat{U}^{-1}(t+i\beta\hbar/2)\hat{U}(t)\hat{\rho},\hat{S}_{\mu}\right]\right\}.\end{aligned} \tag{A5}$$

Next, we consider typical products such as $\hat{U}^{-1}(t)\hat{U}(t \pm i\beta\hbar/2)$ given by

$$\hat{U}^{-1}(t)\hat{U}(t \pm i\beta\hbar/2) = e^{\frac{i}{\hbar}\int_t^{t\pm i\beta\hbar/2}\hat{H}_S(t')dt'}. \tag{A6}$$

In the high temperature limit, we have for the integral

$$\frac{i}{\hbar}\int_t^{t\pm i\beta\hbar/2}\hat{H}_S(t')dt' \approx \mp\frac{\beta}{2}\hat{H}_S(t). \tag{A7}$$

Here we have supposed that the operator $\hat{H}_S(t)$ does not alter significantly during small time increments $\Delta t \sim \beta\hbar/2 \ll 1$. Thus, we can simply take the value of that operator value at time t and consequently may place it outside the integral. By treating in like manner all other such time-dependent functions in Eq. (A5), we have the Hubbard form of the collision kernel equation (A5) with time-dependent Hamiltonian $\hat{H}_S(t)$ which in the high-temperature limit simplifies to Eq. (3). The form of the collision kernel given by Eq. (3) corresponds to the high-temperature limit and short correlation time of the Markovian approximation.

APPENDIX B: MATRIX CONTINUED FRACTION SOLUTION OF EQ. (11)

On introducing the frequency-dependent column vector,

$$\boldsymbol{\rho}_n = \begin{pmatrix} \vdots \\ \boldsymbol{\rho}_n^{-1}(\omega) \\ \boldsymbol{\rho}_n^{0}(\omega) \\ \boldsymbol{\rho}_n^{1}(\omega) \\ \vdots \end{pmatrix} \tag{B1}$$

($n = m + S$), we then have a homogeneous matrix three-term recurrence equation between column vectors $\boldsymbol{\rho}_n$, namely,

$$\mathbf{Q}_n^- \boldsymbol{\rho}_{n-1} + \mathbf{Q}_n \boldsymbol{\rho}_n + \mathbf{Q}_n^+ \boldsymbol{\rho}_{n+1} = \mathbf{0}, \tag{B2}$$

where the matrix elements of the infinite matrices $\mathbf{Q}_n$ and $\mathbf{Q}_n^{\pm}$ are given by

$$[\mathbf{Q}_n]_{kk'} = -i\omega\tau_N k\delta_{kk'} - a_n^+ e^{(2n-2S+1)\frac{\sigma}{S^2}+\frac{\xi_0}{S}} I_{k-k'}\left(\frac{\xi}{2S}\right) - a_n^- e^{-(2n-2S-1)\frac{\sigma}{2S^2}-\frac{\xi_0}{2S}} I_{k-k'}\left(-\frac{\xi}{2S}\right),$$

$$[\mathbf{Q}_n^{\pm}]_{kk'} = a_n^{\pm} e^{\mp(2n-2S\pm1)\frac{\sigma}{2S^2}\mp\frac{\xi_0}{2S}} I_{k-k'}\left(\mp\frac{\xi}{2S}\right).$$

However, a nontrivial solution of the homogeneous Eq. (B2) exists because according to the general method of solution of three-term recurrence relations [25,32], all *higher-order* column vectors $\boldsymbol{\rho}_n$ defined by Eq. (B1) can always be expressed in terms of the *lowest-order* vector column $\boldsymbol{\rho}_0$ via the products

$$\boldsymbol{\rho}_n = \mathbf{S}_n \mathbf{S}_{n-1} \ldots \mathbf{S}_1 \boldsymbol{\rho}_0, \tag{B3}$$

where the $\mathbf{S}_m$ are finite matrix continued fractions defined by the matrix recurrence relation

$$\mathbf{S}_m = [-\mathbf{Q}_m - \mathbf{Q}_m^+ \mathbf{S}_{m+1}]^{-1} \mathbf{Q}_m^-.$$

Now the zero-order column vector ρ_0 itself can be found from the normalization condition for the density matrix elements, viz.,

$$\sum_{n=0}^{2S} \rho_n(t) = \sum_{k=-\infty}^{\infty} \left(\sum_{n=0}^{2S} \rho_n^k(\omega) \right) e^{i\omega k t} = 1, \tag{B4}$$

thereby immediately yielding an *inhomogeneous* equation for $\boldsymbol{\rho}_0$, viz.,

$$\sum_{n=0}^{2S} \boldsymbol{\rho}_n = \mathbf{C}\boldsymbol{\rho}_0 = \mathbf{v}, \tag{B5}$$

where the matrix $\mathbf{C}$ is given by

$$\mathbf{C} = \mathbf{I} + \mathbf{S}_1 + \mathbf{S}_2\mathbf{S}_1 + \cdots + \mathbf{S}_{2S}\cdots\mathbf{S}_2\mathbf{S}_1. \tag{B6}$$

$\mathbf{I}$ is the unit matrix, and the infinite column vector $\mathbf{v}$ has only one nonvanishing element, $v_k = \delta_{k0}$, $-\infty < k < \infty$. Consequently, we have for the zero-order column vector $\boldsymbol{\rho}_0$,

$$\boldsymbol{\rho}_0 = \mathbf{C}^{-1}\mathbf{v}. \tag{B7}$$

Having calculated all the $\boldsymbol{\rho}_0$, we can determine via Eq. (B3) the other column vectors $\boldsymbol{\rho}_n$ as

$$\boldsymbol{\rho}_n = \mathbf{S}_n \mathbf{S}_{n-1} \ldots \mathbf{S}_1 \mathbf{C}^{-1}\mathbf{v}, \tag{B8}$$

and thus we can evaluate all the $S_Z^k(\omega)$ from Eq. (9) yielding the nonlinear stationary ac response of a uniaxial paramagnet.

APPENDIX C: EVALUATION OF THE LONGEST RELAXATION TIME τ

In the absence of the ac driving field, i.e., $\xi = 0$, the recurrence relation, Eq. (5), can be written in the *homogeneous* matrix form

$$\dot{\mathbf{F}}(t) = \Pi \cdot \mathbf{F}(t),$$

where the column vector $\mathbf{F}(t)$ and the tridiagonal system matrix Π are

$$\mathbf{F}(t) = \begin{pmatrix} \rho_0(t) \\ \rho_1(t) \\ \vdots \\ \rho_{2S}(t) \end{pmatrix},$$

$$\Pi = \frac{1}{\tau_N} \begin{pmatrix} p_0 & p_0^+ & 0 & \cdots & 0 \\ p_1^- & p_1 & p_1^+ & \cdots & \vdots \\ \vdots & \vdots & \vdots & \ddots & p_{2S-1}^+ \\ 0 & \cdots & 0 & p_{2S}^- & p_{2S} \end{pmatrix}, \tag{C1}$$

with matrix elements

$$p_n = -\frac{n(2S-n+1)}{2} e^{-(2n-2S+1)\frac{\sigma}{2S^2}-\frac{\xi_0}{2S}} - \frac{(n+1)(2S-n)}{2} e^{(2n-2S+1)\frac{\sigma}{2S^2}+\frac{\xi_0}{2S}},$$

$$p_n^+ = \frac{1}{2}(2S-n)(n+1) e^{-(2n-2S-1)\frac{\sigma}{2S^2}-\frac{\xi_0}{2S}},$$

$$p_n^- = \frac{n}{2}(2S-n+1) e^{(2n-2S-1)\frac{\sigma}{2S^2}+\frac{\xi_0}{2S}}.$$

(These matrix elements are obtained from coefficients $q_m(t)$ and $q_m^{\pm}(t)$ in Eq. (5) by introducing a new index n defined as $n = m + S$). The secular equation, which determines all the eigenvalues, is as usual

$$\det(\Pi - \lambda\mathbf{I}) = 0. \tag{C2}$$

Now the left-hand side of Eq. (C2) represents a polynomial of the order $2S + 1$, viz.,

$$(k_{2S+1}\lambda^{2S} + k_{2S}\lambda^{2S-1} + \cdots + k_2\lambda + k_1)\lambda = 0, \tag{C3}$$

where

$$k_1 = -\sum_{i=0}^{2S} M_i^i, \quad k_2 = \sum_{i=0}^{2S-1} \sum_{j=i+1}^{2S} M_{ij}^{ij},$$

and so on, and we have used the fact that $\det(\boldsymbol{\Pi}) = 0$. Here the $M_i^{i'}$ are the first minors of the matrix $\boldsymbol{\Pi}$, which are the determinants of the square matrices as reduced from $\boldsymbol{\Pi}$ by removing the ith row and the i'th column of $\boldsymbol{\Pi}$ while the $M_{ij}^{i'j'}$ are the minors of the matrix $\boldsymbol{\Pi}$, which are in turn the determinants of the square matrix as reduced from $\boldsymbol{\Pi}$ by

removing *two* (the ith and the jth) of its rows and *two* (the i'th and the j'th) columns. Now in the high-barrier approximation when $\lambda_1 \ll 1$, that quantity can be evaluated analytically by neglecting all higher powers λ^n with $n > 2$ in the secular equation (C3). Thus, we have from that equation,

$$\lambda_1 \approx -\frac{k_1}{k_2}. \tag{C4}$$

However, Eq. (C4) can be equivalently written in matrix form as

$$\lambda_1 \approx \frac{\mathrm{Tr}(\mathbf{M}^{(1)})}{\mathrm{Tr}(\mathbf{M}^{(2)})}, \tag{C5}$$

where $\mathbf{M}^{(1)}$ is the matrix formed from all the first minors,

$$\mathbf{M}^{(1)} = \begin{pmatrix} M_{2S}^{2S} & M_{2S}^{2S-1} & \cdots & M_{2S}^{0} \\ M_{2S-1}^{2S} & M_{2S-1}^{2S-1} & \cdots & M_{2S-1}^{0} \\ \vdots & \vdots & \ddots & \vdots \\ M_{0}^{2S} & M_{0}^{2S-1} & \cdots & M_{0}^{0} \end{pmatrix},$$

and the matrix $\mathbf{M}^{(2)}$ contains all the other $M_{ij}^{i'j'}$ minors,

$$\mathbf{M}^{(2)} = \begin{pmatrix} M_{2S,2S-1}^{2S,2S-1} & M_{2S,2S-1}^{2S,2S-2} & \cdots & M_{2S,2S-1}^{0,0} \\ M_{2S,2S-2}^{2S,2S-1} & M_{2S,2S-2}^{2S,2S-2} & \cdots & M_{2S,2S-2}^{0,0} \\ \vdots & \vdots & \ddots & \vdots \\ M_{0,0}^{2S,2S-1} & M_{0,0}^{2S,2S-2} & \cdots & M_{0,0}^{0,0} \end{pmatrix}.$$

The matrices $\mathbf{M}^{(1)}$ and $\mathbf{M}^{(2)}$ have, respectively, dimensions $n \times n$ and $n(n-1)/2 \times n(n-1)/2$, where $n = 2S+1$. Furthermore, the ordering of the elements of the matrix $\mathbf{M}^{(2)}$ is such that by reading across or down the final matrix, the successive lists of positions appear in lexicographic order. Now the traces $\mathrm{Tr}(\mathbf{M}^{(1)})$ and $\mathrm{Tr}(\mathbf{M}^{(2)})$ can be calculated analytically as

$$\begin{aligned}\mathrm{Tr}(\mathbf{M}^{(1)}) &= \frac{(-1)^{2S}}{\tau_N^{2S}} \sum_{i=0}^{2S} \left[\left(\prod_{s=1}^{i} p_s^- \right) \left(\prod_{r=i}^{2S-1} p_r^+ \right) \right] \\ &= \frac{(2S)!}{2^{2S}\tau_N^{2S}} \sum_{k=-S}^{S} e^{(k^2-S^2)\frac{\sigma}{S^2}+k\frac{\xi_0}{S}} = \frac{(2S)!e^{-\sigma}}{2^{2S}\tau_N^{2S}} Z_S,\end{aligned}$$

and

$$\begin{aligned}\mathrm{Tr}(\mathbf{M}^{(2)}) &= \frac{(-1)^{2S+1}}{\tau_{\mathrm{N}}^{2S-1}} \sum_{i=0}^{2S-1} \sum_{j=i+1}^{2S} \\ &\quad \times \left(\prod_{s=1}^{i} p_s^- \prod_{r=j}^{2S-1} p_r^+ \sum_{m=1}^{j-i} \prod_{u=j+2-m}^{j} p_u^- \prod_{v=i}^{j-m-1} p_v^+ \right) \\ &= \frac{(2S)!e^{-\sigma}}{2^{2S-1}\tau_{\mathrm{N}}^{2S-1}} \sum_{k=-S}^{S-1} \sum_{n=k+1}^{S} \sum_{m=1}^{n-k} \\ &\quad \times \frac{e^{[2k^2-2n-1+2m(2n-m+1)]\frac{\sigma}{2S^2}+(2k+2m-1)\frac{\xi_0}{2S}}}{(S+n-m+1)(S-n+m)}.\end{aligned}$$

Here we have used the result $\prod_{m=a}^{b} p_m^{\pm} = 1$ if $b < a$. Thus in the high-barrier approximation, $\tau/\tau_N \approx \lambda_1^{-1}$ is given by the following approximate equation:

$$\begin{aligned}\tau &\approx \frac{2\tau_N}{Z_S} \sum_{k=-S}^{S-1} \sum_{n=k+1}^{S} \sum_{m=1}^{n-k} \\ &\quad \times \frac{e^{[2k^2-2n-1+2m(2n-m+1)]\frac{\sigma}{2S^2}+(2k+2m-1)\frac{\xi_0}{2S}}}{(S+n-m+1)(S-n+m)}.\end{aligned} \tag{C6}$$

[1] C. D. Mee, *The Physics of Magnetic Recording* (North Holland, Amsterdam, 1986); A.P. Guimarães, *Principles of Nanomagnetism* (Springer, Berlin, 2009).

[2] *Magnetic Nanoparticles*, edited by S. P. Gubin (Wiley, New York, 2009).

[3] Q. A. Pankhurst, N. K. T. Thanh, S. K. Jones, and J. Dobson, Progress in applications of magnetic nanoparticles in biomedicine, J. Phys. D: Appl. Phys. **42**, 224001 (2009).

[4] F. Luis, V. González, A. Millán, and J. L. García-Palacios, Large Quantum Nonlinear Dynamic Susceptibility of Single-Molecule Magnets, Phys. Rev. Lett. **92**, 107201 (2004); R. López-Ruiz, F. Luis, V. González, A. Millán, and J. L. García-Palacios, Nonlinear response of single-molecule nanomagnets: Equilibrium and dynamical, Phys. Rev. B **72**, 224433 (2005); R. López-Ruiz, F. Luis, A. Millán, C. Rillo, D. Zueco, and J. L. García-Palacios, Nonlinear response of single-molecule magnets: Field-tuned quantum-to-classical crossovers, *ibid.* **75**, 012402 (2007).

[5] Yu. L. Raikher and V. I. Stepanov, Nonlinear dynamic susceptibilities and field-induced birefringence in magnetic particle assemblies, Adv. Chem. Phys. **129**, 419 (2004).

[6] T. Bitoh, K. Ohba, M. Takamatsu, T. Shirane, and S. Chikazawa, Linear and nonlinear susceptibilities of ferromagnetic fine particles in Cu97Co3 alloy, J. Phys. Soc. Jpn. **64**, 1311 (1995); Comparative study of linear and nonlinear susceptibilities of fine-particle and spin-glass systems: quantitative analysis based on the superparamagnetic blocking model, J. Magn. Magn. Mater. **154**, 59 (1996).

[7] P. E. Jönsson, T. Jonsson, J. L. García-Palacios, and P. Svedlindh, Nonlinear dynamic susceptibilities of interacting and noninteracting magnetic nanoparticles, J. Magn. Magn. Mater. **222**, 219 (2000); L. Spinu, D. Fiorani, H. Srikanth, F. Lucari, F. D'Orazio, E. Tronc, and M. Noguès, Dynamic studies of γ-Fe2O3 nanoparticle systems, *ibid.* **226**, 1927 (2001); P.E. Jönsson, Superparamagnetism and spin glass dynamics of interacting magnetic nanoparticle systems, Adv. Chem. Phys. **128**, 191 (2004).

[8] Yu. L. Raikher, V. I. Stepanov, A. N. Grigorenko, and P. I. Nikitin, Nonlinear magnetic stochastic resonance: Noise-strength–constant-force diagrams, Phys. Rev. E **56**, 6400 (1997); Yu. L. Raikher and V. I. Stepanov, Noise- and Force-Induced Resonances in Noisy Rotary Oscillations of Classical Spins, Phys. Rev. Lett. **86**, 1923 (2001).

[9] V. A. Ignatchenko and R. S. Gekht, Dynamic hysteresis of a superparamagnet, Zh. Exp. Teor. Fiz. **67**, 1506 (1974) [Sov. Phys. JETP **40**, 750 (1975)].

[10] J. J. Lu, H. L. Huang, and I. Klik, Field orientations and sweep rate effects on magnetic switching of Stoner-Wohlfarth particles, J. Appl. Phys. **76**, 1726 (1994); I. Klik and Y. D. Yao, Hysteresis and limiting cycles in a high frequency ac field, *ibid.* **89**, 7457 (2001).

[11] Yu. L. Raikher, V. I. Stepanov, and R. Perzynski, Dynamic hysteresis of a superparamagnetic nanoparticle, Physica B **343**, 262 (2004); I. S. Poperechny, Yu. L. Raikher, and V. I. Stepanov, Dynamic magnetic hysteresis in single-domain particles with uniaxial anisotropy, Phys. Rev. B **82**, 174423 (2010).

[12] N. A. Usov, Low frequency hysteresis loops of superparamagnetic nanoparticles with uniaxial anisotropy, J. Appl. Phys. **107**, 123909 (2010); J. Carrey, B. Mehdaoui, and M. Respaud, Simple models for dynamic hysteresis loop calculations of magnetic single-domain nanoparticles: Application to magnetic hyperthermia optimization, *ibid.* **109**, 083921 (2011); P. M. Déjardin, Yu. P. Kalmykov, B. E. Kashevsky, H. El Mrabti, I. S. Poperechny, Yu. L. Raikher, and S. V. Titov, Effect of a dc bias field on the dynamic hysteresis of single-domain ferromagnetic particles, *ibid.* **107**, 073914 (2010); J. Carrey, B. Mehdaoui, and M. Respaud, Simple models for dynamic hysteresis loop calculations of magnetic single-domain nanoparticles: Application to magnetic hyperthermia optimization, *ibid.* **109**, 083921 (2011); B. Mehdaoui, J. Carrey, M. Stadler, A. Cornejo, C. Nayral, F. Delpeche, B. Chaudret, and M. Respaud, Influence of a transverse static magnetic field on the magnetic hyperthermia properties and high-frequency hysteresis loops of ferromagnetic FeCo nanoparticles, Appl. Phys. Lett. **100**, 052403 (2012).

[13] D. A. Garanin, Quantum thermoactivation of nanoscale magnets, Phys. Rev. E **55**, 2569 (1997); Density matrix equation for a bathed small system and its application to molecular magnets, Adv. Chem. Phys. **147**, 213 (2011).

[14] D. A. Garanin, Relaxation of superparamagnetic spins: Classical vs large-spin description, Phys. Rev. B **78**, 144413 (2008).

[15] T. Pohjola and H. Schoeller, Spin dynamics of Mn_{12}-acetate in the thermally activated tunneling regime: ac susceptibility and magnetization relaxation, Phys. Rev. B **62**, 15026 (2000).

[16] J. L. García-Palacios and D. Zueco, Solving spin quantum master equations with matrix continued-fraction methods: Application to superparamagnets, J. Phys. A: Math. Gen. **39**, 13243 (2006); D. Zueco and J. L. García-Palacios, Longitudinal relaxation and thermoactivation of quantum superparamagnets, Phys. Rev. B **73**, 104448 (2006).

[17] J. L. García-Palacios and S. Dattagupta, Spin Dynamics in a Dissipative Environment: From Quantal to Classical, Phys. Rev. Lett. **95**, 190401 (2005).

[18] Y. P. Kalmykov, S. V. Titov, and W. T. Coffey, Nonlinear longitudinal relaxation of a quantum superparamagnet with arbitrary spin value S: Phase space and density matrix formulations, Phys. Rev. B **81**, 094432 (2010).

[19] Y. P. Kalmykov, S. V. Titov, and W. T. Coffey, Statistical moment equations for stochastic spin dynamics in phase space: A uniaxial paramagnet subjected to a dc bias field of arbitrary orientation, Phys. Rev. B **86**, 104435 (2012).

[20] Y. P. Kalmykov, S. V. Titov, and W. T. Coffey, Spin-size effects in stochastic resonance in uniaxial superparamagnets, Phys. Rev. B **81**, 172411 (2010); Classical–quantum crossover in magnetic stochastic resonance in uniaxial superparamagnets, J. Phys.: Condens. Matter **22**, 376001 (2010).

[21] Y. Takahashi and F. Shibata, Generalized phase space method in spin systems—Spin coherent state representation, J. Stat. Phys. **14**, 49 (1976); Spin coherent state representation in nonequilibrium statistical mechanics, J. Phys. Soc. Jpn. **38**, 656 (1975).

[22] F. Shibata, Theory of nonlinear spin relaxation, J. Phys. Soc. Jpn. **49**, 15 (1980); F. Shibata and M. Asou, Theory of nonlinear spin relaxation II, **49**, 1234 (1980); F. Shibata and C. Ushiyama, Rigorous solution to nonlinear spin relaxation process, *ibid.* **62**, 381 (1993).

[23] A. M. Perelomov, *Generalized Coherent States and Their Applications* (Springer, Berlin, 1986).

[24] R. R. Puri, *Mathematical Methods of Quantum Optics* (Springer, Berlin, 2001).

[25] W. T. Coffey and Y. P. Kalmykov, *The Langevin Equation*, 3rd ed. (World Scientific, Singapore, 2012).

[26] P. M. Déjardin and Y. P. Kalmykov, Relaxation of the magnetization in uniaxial single-domain ferromagnetic particles driven by a strong ac magnetic field, J. Appl. Phys. **106**, 123908 (2009); S. V. Titov, P.-M. Déjardin, H. El Mrabti, and Y. P. Kalmykov, Nonlinear magnetization relaxation of superparamagnetic nanoparticles in superimposed ac and dc magnetic bias fields, Phys. Rev. B **82**, 100413(R) (2010).

[27] D. A. Varshalovich, A. N. Moskalev, and V. K. Khersonskii, *Quantum Theory of Angular Momentum* (World Scientific, Singapore, 1998).

[28] P. Hubbard, Quantum-mechanical and semiclassical forms of the density operator theory of relaxation, Rev. Mod. Phys. **33**, 249 (1961).

[29] A. G. Redfield, On the theory of relaxation processes, IBM J. Res. Dev. **1**, 19 (1957).

[30] A. Nitzan, *Chemical Dynamics in Condensed Phases: Relaxation, Transfer, and Reactions in Condensed Molecular Systems* (Oxford University Press, New York, 2006).

[31] *Handbook of Mathematical Functions*, edited by M. Abramowitz and I. A. Stegun (Dover, New York, 1972).

[32] H. Risken, *The Fokker-Planck Equation*, 2nd ed. (Springer-Verlag, Berlin, 1989).

[33] Y. P. Kalmykov, W. T. Coffey, and S. V. Titov, Analytic calculation of the longitudinal dynamic susceptibility of uniaxial superparamagnetic particles in a strong uniform dc magnetic field, J. Magn. Magn. Mater. **265**, 44 (2003); Y. P. Kalmykov and S. V. Titov, Calculation of longitudinal susceptibility of superparamagnetic particles, Fiz. Tverd. Tela (S.P-eterburg) **45**, 2037 (2003) [Sov. Phys. Solid State **45**, 2140 (2003)].